Article

Not peer-reviewed version

Activities of some cannabinoids as predicted by molecular docking computation and confirmed by cell calcium assay

Bardia Shahbod , Sepehr Roonasi , Abolfazl Rahimi , Paul C.H. Li *

Posted Date: 27 January 2026

doi: 10.20944/preprints202601.2096.v1

Keywords: cannabis; cannabinoids; cell calcium; microplate fluorescence assay; molecular docking

 doi:10.20944/preprints202601.2096.v1

Article

Activities of Some Cannabinoids as Predicted by Molecular Docking Computation and Confirmed by Cell Calcium Assay

Bardia Shahbod, Sepehr Roonasi, Abolfazl Rahimi and Paul C.H. Li *

Department of Chemistry, Simon Fraser University, 8888 University Drive, Burnaby, British Columbia, Canada
* Correspondence: paulli@sfu.ca

Abstract

Many cannabinoids are derived from *Cannabis* and exhibit a diverse range of pharmacological properties. Predictions of bioactivities of these compounds were conducted by molecular docking computation on two transient receptor potential (TRP) receptors (TRPV1 and TRPC5) found on human glioma (U-87 MG) cells. These predictions were experimentally confirmed by monitoring changes in intracellular calcium concentration $[Ca^{2+}]_i$ in U-87 MG cells treated with cannabinol (CBN), cannabichromene (CBC), and cannabicyclol (CBL), as measured using a fluorescence microplate reader. The results indicate that CBN and CBC are bioactive, whereas CBL exhibits minimal activity. These findings are consistent with predictions obtained from molecular docking computation based on AutoDock Vina.

Keywords: cannabis; cannabinoids; cell calcium; microplate fluorescence assay; molecular docking

Introduction

The global demand for medical-grade *Cannabis* has drastically increased patient interest in the use of cannabinoid-based substances. Due to their limited psychoactivity, cannabinoids such as CBN and CBL have demonstrated efficacy in several pathological conditions, including inflammatory and neurodegenerative diseases, epilepsy, autoimmune disorders such as multiple sclerosis and arthritis, schizophrenia, and cancer [1]. Cannabinoids have been reported to trigger TRPV-dependent autophagic processes in glioma stem-like cells, thereby abolishing chemoresistance to carmustine [3]. In addition, combinations of cannabinoids with cytotoxic drugs such as temozolomide, carmustine, or doxorubicin have been shown to enhance drug activity and uptake in human glioblastoma multiforme (GBM) cells [2].

Cannabinoids have also been demonstrated to modulate glioma progression through multiple mechanisms, including regulation of cell proliferation, invasion, apoptosis, and autophagy pathways, independent of classical cannabinoid receptors [6,19–21].

Beyond pharmacological characterization, cell-based biosensing and cell-monitoring assays enable quantitative detection of functional intracellular responses to chemical stimuli. Intracellular calcium is a robust biosensing parameter that reflects ion channel activity and downstream signaling, and fluorescence microplate monitoring provides a convenient route to high-throughput functional sensing. In this work, we adopt the Fluo-4 microplate assay as a cell-monitoring biosensing platform, and we integrate it with molecular docking to guide compound selection and interpretation.

GBM is the most common and aggressive malignant brain tumor, accounting for approximately 50% of all gliomas and 15.6% of all primary brain and central nervous system tumors [4,5]. Calcium-permeable transient receptor potential (TRP) channels play a critical role in glioma cell proliferation and translocation. In particular, TRPC1 has been shown to be a prerequisite for glioma cell proliferation and migration [7,9,11]. Elevated expression levels of TRPV1, TRPV2, TRPC1, TRPC6, TRPM2, TRPM3, TRPM7, and TRPM8 have also been reported in GBM tissues [12].

 doi:10.20944/preprints202601.2096.v1

Beyond TRPV and TRPC channels, intracellular calcium signaling plays a central role in glioma cell survival, migration, and neuroprotection, making calcium homeostasis an attractive therapeutic target in cancer research [8,10,13]. Several studies have demonstrated that non-psychoactive cannabinoids such as cannabidiol can induce apoptosis, inhibit proliferation, and suppress invasion in glioma and other cancer cell lines through multi-target mechanisms [22–28]. Cannabinoids have also been reported to directly interact with TRP channels, including TRPV1, thereby regulating intracellular calcium dynamics and downstream signaling pathways associated with tumor progression [29–32].

Targeting calcium channel activity and intracellular calcium accumulation has therefore emerged as a promising strategy for cancer therapy. The present study was designed to investigate the pharmacological potential of selected cannabinoids in U-87 MG glioma cells based on intracellular calcium measurements. Previous studies have reported significant calcium changes in U-87 MG cells treated with curcumin [33,34], resveratrol [34], and capsaicin [34]. Predictions were also obtained using molecular docking computations based on AutoDock Vina, and a strong correlation between intracellular calcium measurements and molecular docking predictions has been previously established [34].

Experimental Section

Reagents

A fluorescent calcium probe, Fluo-4 AM ester (50 μg, Molecular Probes, Eugene, OR) was dissolved in dimethyl sulfoxide (DMSO, 99.9%, Sigma–Aldrich) to prepare a stock solution of 1 μg μL^{-1}. Prior to use, the stock solution was freshly diluted in Hanks' balanced salt solution (HBSS, Invitrogen Corp., Grand Island, NY) to yield a working concentration of 5.0 μM. Due to its light sensitivity, Fluo-4 AM was stored in the dark at −20 °C [15].

Cannabinol (CBN), cannabichromene (CBC), and cannabicyclol (CBL) were purchased from Cerilliant Corporation (Round Rock, TX) as drug enforcementa-exempt solutions (1 mg mL^{-1} in methanol).

Ionomycin calcium salt (Sigma Chemical Co.) was dissolved in DMSO and diluted in HBSS containing 1 mM $CaCl_2$ to prepare working solutions of 10 mg mL^{-1} [14].

Cell Samples

U-87 MG cells (ATCC, USA) were obtained from cryopreserved storage and were maintained in DMEM/high glucose, pyruvate (ThermoFisher Scientific), containing 10% FBS (ThermoFisher Scientific), and 1% penicillin (Stemcell Technologies) in a 5% CO_2 atmosphere at 37 °C. The doubling time for the cell line was approximately 39 h; hence, the growth medium was changed two times a week, and cells were passaged once a week. We used 0.05% trypsin-EDTA (ThermoFisher Scientific) to detach cells, and 0.4% trypan blue solution (ThermoFisher Scientific) to ensure the viability of the cell under the microscope. Dead cells will become stained after the addition of trypan blue and live cells can be observed as bight circles.

Instrument

Fluorescence measurements were performed using a microplate reader (M200, Tecan, Switzerland). Intracellular calcium concentration was calculated using the following equation 1 [17]:

$$[Ca^{2+}]_i = K_d \frac{F - F_{min}}{F_{max} - F} \qquad \text{(Equation 1)}$$

where F represents fluorescence intensity after reagent addition, F_{min} is the background fluorescence, and F_{max} is the maximum fluorescence obtained following ionomycin treatment. The dissociation constant (K_e) for Fluo-4 is 0.35 μM [18].

 doi:10.20944/preprints202601.2096.v1

Cell Calcium Bulk Analysis

Bulk analysis of intracellular calcium was performed using a 96-well microplate coupled with fluorescence detection. This method enables rapid and reproducible measurement of cytosolic calcium changes following chemical stimulation. The overall experimental workflow is illustrated schematically in Figure 1.

Figure 1. Different steps of cell calcium bulk analysis.

3.2. Loading Cells on a 96-Well Plate

After reaching adequate confluency, cells were detached using trypsin-EDTA. A 50 µL aliquot of cell suspension was mixed with 50 µL of trypan blue solution and counted using a hemocytometer. Live cells were identified as unstained bright circular objects under microscopic observation. Cell density was calculated using standard hemocytometer protocols, and 10 000 viable cells were seeded into each well of a black, clear-bottom 96-well cell culture plate. Plates were incubated overnight to allow cell attachment.

3.3. Fluo-4 AM Dye Loading

After cell attachment, the culture medium was removed and cells were washed with HBSS. Fluo-4 AM working solution (5.0 µM, 20 µL per well) was added, followed by incubation for 15 min at room temperature and an additional 15 min at 37 °C to allow dye uptake and intracellular ester hydrolysis. Excess dye was removed by washing with HBSS prior to fluorescence measurements.

3.4. Fluorescence Assay on a 96-Well Plate

Fluorescence measurements were performed in a black, clear-bottom COC-coated 96-well plate at a cell density of 10 000 cells per well. Measurements were carried out using the bottom-reading mode with fluorescence excitation at 470 nm and emission at 530 nm. Instrument settings included 25 flashes and an integration time of 20 µs. The fluorescence gain was maintained between 170 and 190, and they were corrected for Fmin, F and Fmax obtained in each experiment, by the relationship between fluorescence intensity and gain as depicted in Figure 2.

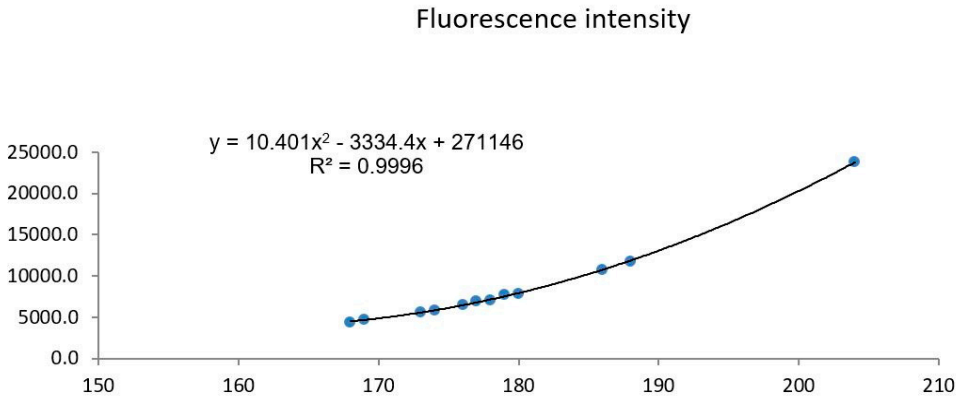

Figure 2. Relationship between fluorescent intensity and microplate reader gain.

 doi:10.20944/preprints202601.2096.v1

Fluorescence intensity was recorded in three stages: resting fluorescence (F_0), fluorescence after reagent addition (F), and maximal fluorescence (F_{max}) following ionomycin treatment (final concentration 20 μM). This three-point acquisition provides a rapid functional readout of stimulus-invoked Ca^{2+} responses suitable for cell monitoring and screening in a microplate format. Background fluorescence (F_{min}) was measured in cell-free wells. All experiments were performed in triplicate. Data are reported as mean ± standard deviation (SD), and fold-change was calculated relative to resting [Ca^{2+}] for each condition.

Data Analysis and Results

The intracellular Ca^{2+} biosensing assay produced a clear functional dynamic range across the tested cannabinoids, with fold responses spanning from minimal change (CBL) to strong activation (CBN/CBC). Measurements were performed in triplicate, and the low SD values indicate good reproducibility of the microplate fluorescence readout under constant instrument settings (gain correction). These characteristics support the use of the assay as a cell-monitoring biosensor for screening stimulus-evoked Ca^{2+} responses. Changes in intracellular calcium concentration were calculated using Equation (1). Calcium concentrations (nM) and fold changes relative to resting levels are summarized in Table 1. CBC and CBN induced pronounced increases in intracellular calcium concentration, whereas CBL produced only minimal changes.

To correlate the computational prediction with the cell-monitoring readout, molecular docking was used as a screening and ranking tool for TRPV1 and TRPC5 channels. The cannabinoids CBN and CBC showed stronger predicted binding affinities than CBL across the tested channel structures (Table 2), and this ranking correlated with the experimental calcium responses (Table 1), where CBN/CBC produced pronounced Ca^{2+} elevations and CBL showed minimal effect. The predicted channel binding poses and interaction patterns are summarized in Figures 3 and 4, supporting a mechanistic interpretation consistent with the biosensing results.

Table 1. Changes in [Ca^{2+}] when 100 μM of reagents (CBC, CBN, CBL) were added.

Compound	Resting [Ca^{2+}] (nM)	After Treatment [Ca^{2+}] (nM)	Fold Increase
CBN	445 ± 8	2144 ± 47	4.8
CBC	463 ± 6	2295 ± 31	4.9
CBL	311 ± 40	361 ± 15	1.2

Table 2. Binding affinity of different cannabinoids on two major TRPV1 ion channels (of rat and human origins).

Ion Channel	PDB ID	CBC (kcal/mol)	CBL (kcal/mol)	CBN (kcal/mol)
Rat TRPV1	3J5Q	−5.7	−6.0	−5.2
Rat TRPV1	3J5R	−7.6	−8.3	−8.3
Human TRPV1	6L93	−7.4	−7.9	−8.0
Human TRPC5	6YSN	−4.2	−4.5	−5.0±

(a)

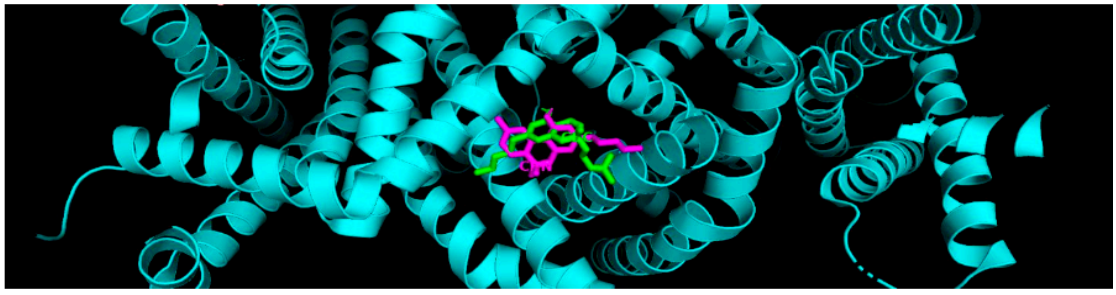

 doi:10.20944/preprints202601.2096.v1

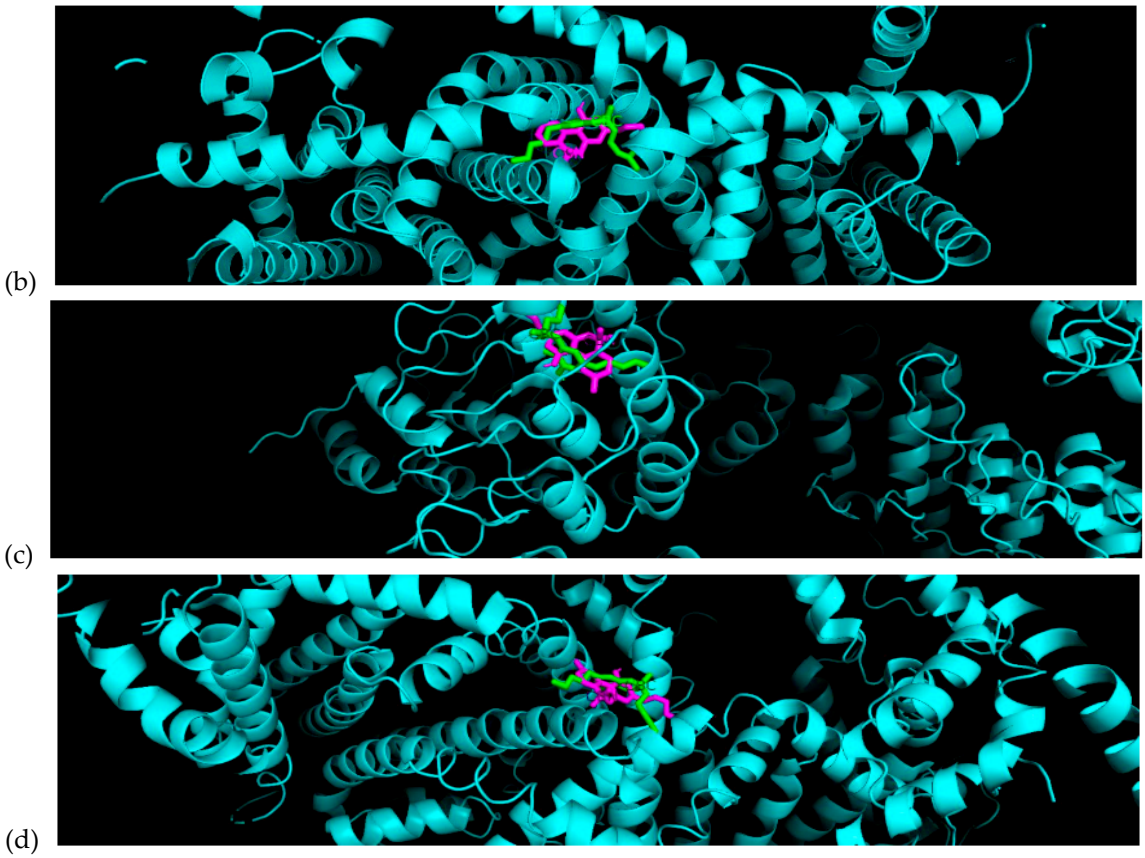

Figure 3. Predicted docking poses of cannabinoids in TRP ion channels generated using Autodock Vina. (a) Rat TRPV1 (PDB ID: 3J5Q), (b) Rat TRPV1 (PDB ID: 3J5R), (c) Human TRPV1 (PDB ID: 6L93), (d) Human TRPC5 (PDB ID: 6YSN). Receptor structures are shown in cyan ribbon representation, and cannabinoid ligands are shown in magenta stick format. In all cases, the ligands occupy the hydrophobic transmembrane binding pockets consistent with known ligand interaction regions, supporting a potential modulatory role in calcium-permeable channels.

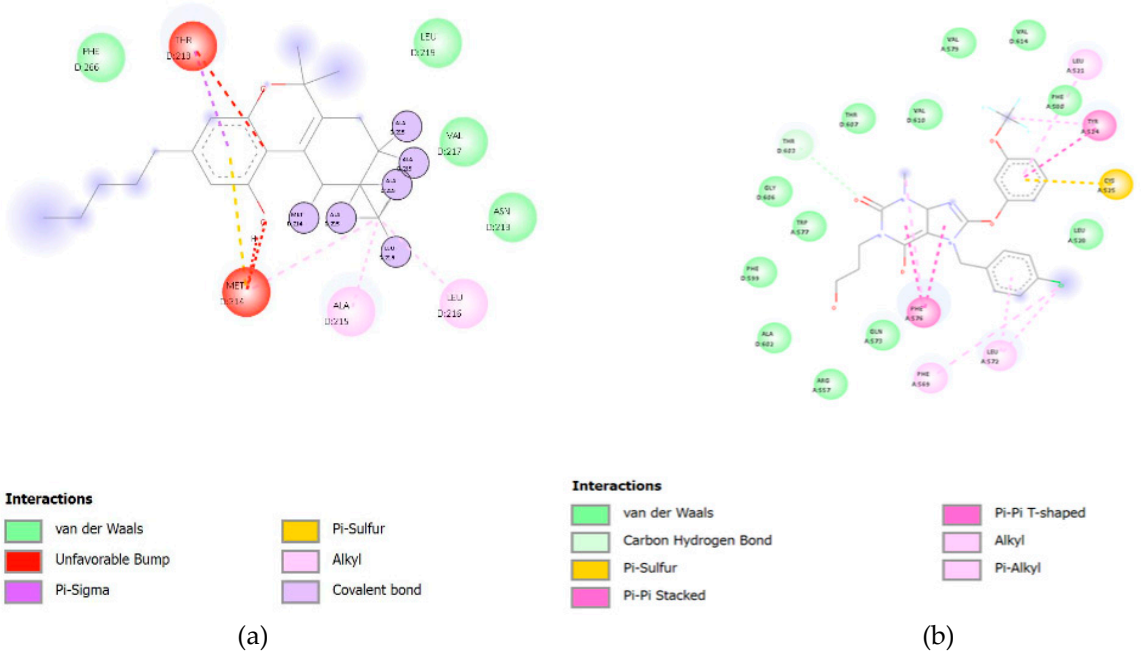

(a) (b)

Figure 4. Two-dimensional interaction maps illustrating predicted molecular contacts and interactions between cannabinol (CBN) and human TRP channels. (a) Human TRPV1 (PDB ID: 6L93), (b) Human TRPC5 (PDB ID:

 doi:10.20944/preprints202601.2096.v1

6YSN). These molecular interaction maps provide structural context that supports the experimentally observed Ca^{2+} responses obtained from the cell-monitoring assay.

Conclusion

A fluorescence-based intracellular calcium assay was implemented as a cell-monitoring biosensing platform to evaluate cannabinoid-induced functional responses in U-87 MG glioma cells. CBC and CBN produced pronounced intracellular Ca^{2+} elevations, whereas CBL induced minimal responses, demonstrating the assay's ability to discriminate bioactivity based on functional signaling output. The strong agreement between experimental Ca^{2+} readouts and molecular docking predictions highlights the value of integrating computational screening with cell-based biosensing as an efficient workflow for identifying bioactive compounds.

Author Contributions: conceptualization, PL; methodology, PL, BS, SR, AR; formal analysis, PL, BS, SR, AR; investigation, PL, BS, SR, AR; resources, PL; writing-original, BS, SR, AR, writing-review, PL, BS, SR, AR; supervision, PL; project admin, PL; funding acquisition, PL.

Funding: Funding by NSERC of Canada as said in the paper, grant number is RGPIN-2022-03320

Institutional Review Board Statement: Not applicable

Informed Consent Statement: Not applicable

Data Availability Statement: The original contributions presented in this study are included in the article. Further inquiries can be directed to the corresponding author(s).

Acknowledgments: We thank the funding from Natural Sciences and Engineering Research Council of Canada.

Conflicts of Interest: The authors declare no conflict of interest

References

1. Pisanti S, Malfitano AM, Ciaglia E, Lamberti A, Ranieri R, Cuomo G, et al. Cannabidiol: State of the art and new challenges for therapeutic applications. Pharmacology & therapeutics. 2017;175:133-50.
2. Nabissi M, Morelli MB, Santoni M, Santoni G. Triggering of the TRPV2 channel by cannabidiol sensitizes glioblastoma cells to cytotoxic chemotherapeutic agents. Carcinogenesis. 2013;34(1):48-57.
3. Nabissi M, Morelli MB, Amantini C, Liberati S, Santoni M, Ricci-Vitiani L, et al. Cannabidiol stimulates Aml-1a-dependent glial differentiation and inhibits glioma stem-like cells proliferation by inducing autophagy in a TRPV2-dependent manner. International journal of cancer. 2015;137(8):1855-69.
4. Rice T, Lachance DH, Molinaro AM, Eckel-Passow JE, Walsh KM, Barnholtz-Sloan J, et al. Understanding inherited genetic risk of adult glioma – a review. Neuro-Oncology Practice. 2015;3(1):10-6.
5. Dumitru CA, Sandalcioglu IE, Karsak M. Cannabinoids in Glioblastoma Therapy: New Applications for Old Drugs. Frontiers in molecular neuroscience. 2018;11:159.
6. Velasco G, Carracedo A, Blázquez C, Lorente M, Aguado T, Haro A, et al. Cannabinoids and gliomas. Molecular neurobiology. 2007;36(1):60-7.
7. Nimmrich V, Gross G. P/Q-type calcium channel modulators. Br J Pharmacol. 2012;167(4):741-59.
8. Montana V, Sontheimer H. Bradykinin promotes the chemotactic invasion of primary brain tumors. The Journal of neuroscience : the official journal of the Society for Neuroscience. 2011;31(13):4858-67.
9. Watkins S, Sontheimer H. Unique biology of gliomas: challenges and opportunities. Trends in neurosciences. 2012;35(9):546-56.
10. Bomben VC, Sontheimer HW. Inhibition of transient receptor potential canonical channels impairs cytokinesis in human malignant gliomas. Cell proliferation. 2008;41(1):98-121.
11. Cuddapah VA, Turner KL, Sontheimer H. Calcium entry via TRPC1 channels activates chloride currents in human glioma cells. Cell calcium. 2013;53(3):187-94.

 doi:10.20944/preprints202601.2096.v1

12. Alptekin M, Eroglu S, Tutar E, Sencan S, Geyik MA, Ulasli M, et al. Gene expressions of TRP channels in glioblastoma multiforme and relation with survival. Tumour biology : the journal of the International Society for Oncodevelopmental Biology and Medicine. 2015;36(12):9209-13.
13. Duncan RS, Goad DL, Grillo MA, Kaja S, Payne AJ, Koulen P. Control of intracellular calcium signaling as a neuroprotective strategy. Molecules (Basel, Switzerland). 2010;15(3):1168-95.
14. Li X, Li PC. Microfluidic selection and retention of a single cardiac myocyte, on-chip dye loading, cell contraction by chemical stimulation, and quantitative fluorescent analysis of intracellular calcium. Analytical chemistry. 2005;77(14):4315-22.
15. Li X, Xue X, Li PCH. Real-time detection of the early event of cytotoxicity of herbal ingredients on single leukemia cells studied in a microfluidic biochip. Integrative Biology. 2009;1(1):90-8.
16. Huang, H. C., P. Chang, S. Y. Lu, B. W. Zheng, and Z. F. Jiang. 2015. Protection of curcumin against amyloid-beta-induced cell damage and death involves the prevention from NMDA receptor-mediated intracellular Ca^{2+} elevation. *Journal of receptor and signal transduction research* 35 (5):450-7. doi: 10.3109/10799893.2015.1006331.
17. Takahashi, A., P. Camacho, J. D. Lechleiter, and B. Herman. 1999. Measurement of intracellular calcium. *Physiological Reviews* 79 (4):1089-125. doi: 10.1152/physrev.1999.79.4.1089.
18. Gee KR, Brown KA, Chen WN, Bishop-Stewart J, Gray D, Johnson I. Chemical and physiological characterization of fluo-4 Ca(2+)-indicator dyes. Cell calcium. 2000;27(2):97-106.
19. Fraguas-Sánchez AI, Martín-Sabroso C, Torres-Suárez AI. Insights into the effects of the endocannabinoid system in cancer: a review. Br J Pharmacol. 2018;175(13):2566-80.
20. Hinz B, Ramer R. Anti-tumour actions of cannabinoids. Br J Pharmacol. 2019;176(10):1384-94.
21. Ramer R, Hinz B. Cannabinoids as Anticancer Drugs. Advances in pharmacology (San Diego, Calif). 2017;80:397-436.
22. Ligresti A, Moriello AS, Starowicz K, Matias I, Pisanti S, De Petrocellis L, et al. Antitumor activity of plant cannabinoids with emphasis on the effect of cannabidiol on human breast carcinoma. The Journal of pharmacology and experimental therapeutics. 2006;318(3):1375-87.
23. Shrivastava A, Kuzontkoski PM, Groopman JE, Prasad A. Cannabidiol induces programmed cell death in breast cancer cells by coordinating the cross-talk between apoptosis and autophagy. Molecular cancer therapeutics. 2011;10(7):1161-72.
24. Sultan AS, Marie MA, Sheweita SA. Novel mechanism of cannabidiol-induced apoptosis in breast cancer cell lines. Breast (Edinburgh, Scotland). 2018;41:34-41.
25. Massi P, Vaccani A, Ceruti S, Colombo A, Abbracchio MP, Parolaro D. Antitumor effects of cannabidiol, a nonpsychoactive cannabinoid, on human glioma cell lines. The Journal of pharmacology and experimental therapeutics. 2004;308(3):838-45.
26. Vaccani A, Massi P, Colombo A, Rubino T, Parolaro D. Cannabidiol inhibits human glioma cell migration through a cannabinoid receptor-independent mechanism. Br J Pharmacol. 2005;144(8):1032-6.
27. Massi P, Valenti M, Vaccani A, Gasperi V, Perletti G, Marras E, et al. 5-Lipoxygenase and anandamide hydrolase (FAAH) mediate the antitumor activity of cannabidiol, a non-psychoactive cannabinoid. Journal of neurochemistry. 2008;104(4):1091-100.
28. Solinas M, Massi P, Cinquina V, Valenti M, Bolognini D, Gariboldi M, et al. Cannabidiol, a non-psychoactive cannabinoid compound, inhibits proliferation and invasion in U87-MG and T98G glioma cells through a multitarget effect. PloS one. 2013;8(10):e76918.
29. De Petrocellis L, Ligresti A, Moriello AS, Allarà M, Bisogno T, Petrosino S, et al. Effects of cannabinoids and cannabinoid-enriched Cannabis extracts on TRP channels and endocannabinoid metabolic enzymes. Br J Pharmacol. 2011;163(7):1479-94.
30. Bisogno T, Hanus L, De Petrocellis L, Tchilibon S, Ponde DE, Brandi I, et al. Molecular targets for cannabidiol and its synthetic analogues: effect on vanilloid VR1 receptors and on the cellular uptake and enzymatic hydrolysis of anandamide. Br J Pharmacol. 2001;134(4):845-52.
31. Lu J, Ju YT, Li C, Hua FZ, Xu GH, Hu YH. Effect of TRPV1 combined with lidocaine on cell state and apoptosis of U87-MG glioma cell lines. Asian Pacific journal of tropical medicine. 2016;9(3):288-92.

 doi:10.20944/preprints202601.2096.v1

32. Kárai LJ, Russell JT, Iadarola MJ, Oláh Z. Vanilloid receptor 1 regulates multiple calcium compartments and contributes to Ca2+-induced Ca2+ release in sensory neurons. The Journal of biological chemistry. 2004;279(16):16377-87.
33. Hamideh Sharifi Noghabi, Abdul Q. Ahmed, and Paul C. H. Li. Intracellular Calcium Increases due to Curcumin Measured using a Single-Cell Biochip. Anal. Lett. 54, **2021**, 2769-2776.
34. Natali Pflaum-Jaeger, Bardia Shahbod, Abolfazl Rahimi, Paul C.H. Li, "Responses to herbal compounds in brain cancer cells: two cell-calcium assays and a molecular docking computation study," Anal. Lett. 2025, 58, 2338-2350.